

Representative Value of Thermal Conductivity for Wickless Heat Pipe in a Thermoelectric Generator System via Computational Numerical Analysis

N. F. Zamri*, A. N. Rahin and M. H. Hamdan

School of Mechanical Engineering, College of Engineering, Universiti Teknologi MARA, 40450, Shah Alam, Selangor, Malaysia

*corresponding author: nurfaraninizamri@gmail.com

ABSTRACT

Thermoelectric generator (TEG) cells are capable of producing electricity from the flow of heat through semiconductor materials via the Seebeck effect. A TEG module (TEM) was developed through the integration of TEG cells, heat pipes, and heat sinks with the function to recover low-temperature waste heat for combined heat and power outputs. The mechanics of heat transport through the components have a distinctive impact on overall performance. In analytical assessment, heat transfer coefficient of heat pipe is usually replaced with thermal conductivity as it is critical to evaluate the boiling and condensation of the working fluid. The thermal conductivity represents the overall behaviour of the heat pipe in transferring heat. Computational numerical analysis simplifies the structure of heat pipe without considering the internal design and modelling it as a solid copper rod. To determine the representative thermal conductivity of the wickless heat pipe, a computational numerical model of the TEM was developed. Experiment data of the TEM operation was used to validate the computational model where the cold-side air inlet temperature inlet was 20.7°C while the hot-side waste heat inlet temperature was 70.0°C. The representative thermal conductivity value for the wickless heat pipe was found to be 500 W/m.K in which the percentage difference for the hot-side and cold-side TEG surface temperatures, and the TEG surface temperature difference were below 5%. The approach was proven suitable to analyse the representative heat pipe thermal conductivity for simplified thermoelectric generator modules.

Keywords: thermoelectric generator; heat pipe; waste heat; thermal conductivity

Nomenclature (Greek symbols towards the end)

ρ	Density
$T_{TEG,H}$	TEG hot surface temperature
$T_{TEG,C}$	TEG cold surface temperature
T_{HO}	Hot outlet temperature
T_{HI}	Hot inlet temperature
T_{CO}	Cold outlet temperature
T_{CI}	Cold inlet temperature
k_{TEG}	Thermoelectric generator thermal conductivity
k_{HP}	Heat pipe thermal conductivity
k	Thermal conductivity
C_p	Specific heat
ΔT	TEG surfaces temperature difference

Abbreviations

CFD	Computational fluid dynamics
CHP	Combined heat and power
HP	Heat pipe
HS	Heat sink
TEG	Thermoelectric generator
TEM	Thermoelectric generator module

1.0 INTRODUCTION

Thermal-to-electrical energy conversion of industrial waste heat using thermoelectric generators (TEG) is a huge prospect to increase energy utilization efficiency. A TEG cell is an energy converter comprising of solid-state semiconductor materials that excite free electrons proportionately to the flow of thermal energy. Electrical

power is generated if the TEG cells are positioned between a heat source and a heat sink [1]. TEG technology has the advantage of being small in size and requires no maintenance [2]. However, the current conversion efficiency of the TEG is less than 5% [3], but progress in semiconductor materials exhibiting the Seebeck effect have seen the development of TEG cells with higher temperature-independent figure-of-merit (ZT) and efficiencies reaching 20% under lab-test conditions [4]. Progress in TEG cell efficiency indicates that direct power production by utilizing industrial waste heat energy is economically viable and practical in the near future.

TEG cells are usually integrated with a heat exchanger system and referred to as a thermoelectric module (TEM). A TEM absorbs heat from a hot waste stream, allows the heat to flow effectively across the TEG cells, and then dissipates the heat to a cooler fluid stream. As the electrical power generation in the TEG cells is proportionate to the heat transfer rate across the cells, a large temperature difference between the opposite surfaces of the TEG is needed. Therefore, a TEM design is built with three sub-sections to promote effective heat transfer across the hot and cold streams – two sections of heat exchangers connected via heat pipes to a section housing the TEG cells [5].

Heat pipes are passive devices that utilize the evaporating and condensing concept of an internal working fluid to obtain heat transfer rates higher than conduction through solid metals [6]. Basically, a heat pipe is a hollow cylinder filled with working fluid and the boiling-condensing processes continue as long as there is a temperature difference at both ends. It is useful for long-distance heat transport with the minimal heat loss, which is an important aspect in the logistics and techno economics of energy recovery system designs. Heat pipes are scalable to fit compact heat exchanger designs, with other advantages such as being light weight, economical and high reliability [7]. The thermal conductivity and efficiency of heat pipe depend on the internal structure and working fluid of the device. Wickless or thermosyphon heat pipe is the simplest form and gravity assisted type while wickless heat pipes contain capillary structure at the inner wall to transport working fluid from the condenser section back to evaporator section. A study conducted by Arun et al. compared thermosyphon and grooved heat pipe as low heat loads are applied. The study concluded that grooved heat pipe design has an efficiency of 81%, which is 7% higher than ordinary wickless heat pipes [8].

A potential use of TEM is for combined heat and power (CHP) applications. Mahdi et al. [9] generated 12.2 W of electricity using 3 TEG cells from the waste heat of a kerosene stove. Simultaneously, 235 W of energy transfer was also obtained to heat household water by 28°C. Other TEM designs for CHP are nanostructured bulk TEG cells for a residential gas-fired condensing boiler [10], the work of Zarifi et al. [11] in recovering waste heat from an economizer, and a TEM CHP system for low-grade waste heat by Zhou et al. [12] using 30 TEG cells for domestic water heating. In their designs, the combination of heat pipes and heat sinks to capture and transfer heat effectively across the system have been proven to be successful, and this is a very essential aspect especially for low-temperature waste heat streams [13].

To assess the practical use of unique TEM systems, modelling of the TEM system performance is essential due to the unique geometrical and operating parameters of each design and application. An important parameter in the analytical model of TEM systems is the convection heat transfer coefficient during the boiling and condensation of the working fluid (normally water) within the heat pipes. However, the convection coefficient value is normally replaced by a representative thermal conductivity value of the heat pipe [14].

A new TEM incorporating two TEG cells, two finned-plate heat sinks and twelve heat pipes was developed and tested based on the operation of a waste heat recovery from bakery ovens in a bread-making factory. In order to develop an accurate analytical model of the TEM, the representative value of the wickless heat pipes thermal conductivity needs to be obtained as a simplified modelling approach replacing the more complex convection mechanics occurring within the heat pipes. This manuscript reports the computational fluid dynamics model of the TEM that was developed to specifically determine the representative value of the heat pipe thermal conductivity, based on the validations made with the available experiment data. The reported work is useful in the field of TEM design and operation for CHP since the representative thermal conductivity value of the heat pipes is sensitive and unique to its operating conditions. In a TEM WHR system, the addition of heat pipes is crucial to prevent heat loss for optimum heat transfer and temperature difference between TEG surfaces. By modelling and obtaining the representative value of thermal conductivity for the heat pipes, the inaccuracy and flaws of the TEM system could be avoided and adjusted. Additionally, by conducting numerical analysis and obtaining the representative thermal conductivity value, the complex consideration for the boiling and condensation principle of heat pipes could be replaced with a more understandable mathematical analysis. Therefore, the presented approach would allow the performance of the heat pipes used in the TEM design to be critically evaluated.

2.0 METHODOLOGY

2.1 Physical configurations

A TEM is physically developed for the purpose of waste heat recovery based on the operating conditions of an industrial bread-baking oven. As shown Figure 1, it primarily consists of TEG cells, finned heat sinks, heat pipes and a copper block. The design consists of two TEG cells to convert the waste heat into direct current electricity. The TEG cells are positioned and clamped between two copper blocks, where each block is connected

to six heat pipes. The heat pipes are attached to a heat sink, designed with sixty plates of aluminium fins. Table 1 provides the list of specifications for each TEM components.

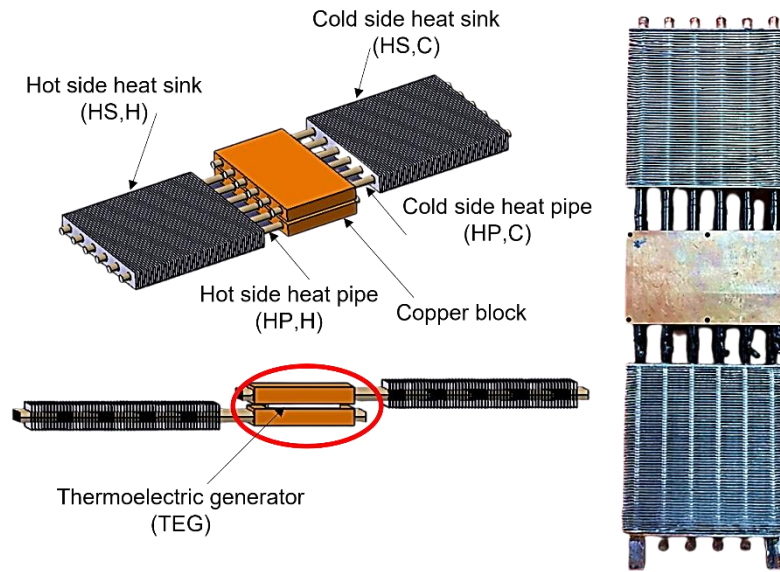


Figure 1. The Thermoelectric Generator Module (TEM) design

Figure 2 summarizes the numerical study reported in this manuscript. Before developing the numerical model of the TEM system, an actual lab-scale testing is conducted. The actual test bench setup is shown in **Figure 3**. In the experimental work, electric heater is used to imitate the waste heat stream at 70°C, assisted by an industrial blower to control the speed. Data logger is used for temperature data displaying and recording as external loads are applied to TEG cells. The data logger is also used for real-time temperature monitoring to ensure the system has reached steady-state condition before the actual data collection. The aim of the study is to determine the representative value of thermal conductivity of heat pipes by comparing the temperature of the hot and cold surfaces of TEG cells. The temperature data collected from the experimental work is sufficient for comparison with the CFD model developed.

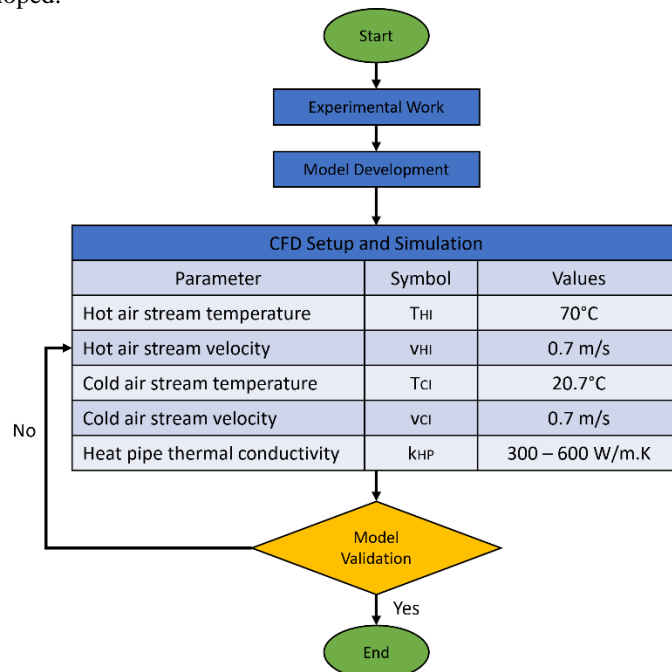


Figure 2. Flow of the Computational Numerical Study of TEM system

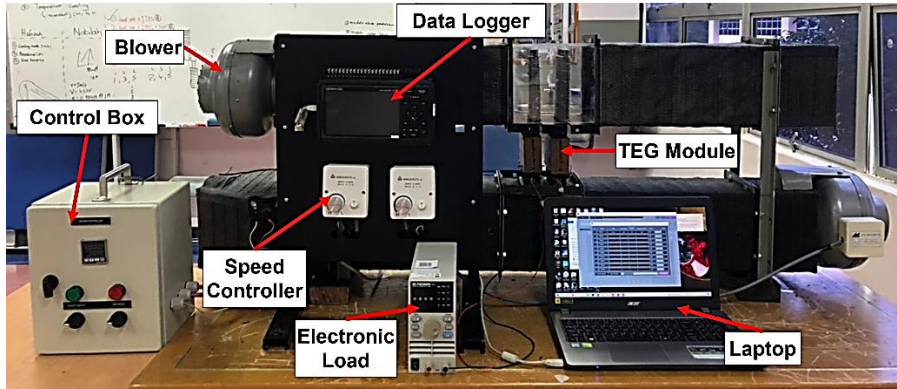


Figure 3. Experimental setup for the WHR system

Table 1: Specifications of the TEM components

Component	Specification details	Functions
Thermoelectric generator (TEG) cell	62 mm x 3.85 mm x 62 mm Number of TEG : 2 TEGs	To convert thermal energy to electrical energy using the Seebeck effect
Copper Block	154 mm x 15 mm x 87 mm Number of copper block: 2 copper blocks	Serve as base plate sandwiching the two TEGs
Heat pipes	Diameter, D: 9 mm Length, L: 300 mm Number of heat pipes : 6 units for each heat sink	To transport heat through the TEG module system
Heat sinks	Rectangular 154 mm x 22 mm x 146 mm Number of fins: 60 fins per heat sink	To capture the waste heat for hot side and dissipate heat at cold side

The TEM is developed to function as a CHP system (refer Figure 4). The waste thermal energy from the main baking oven is absorbed by the hot-side heat sink and transferred through the heat pipes, copper block and TEG to the cold-side heat exchanger, where the waste energy is dissipated to pre-heat a cold air stream before it enters the proofing oven of the bread-baking operation. Electrical power generation by the TEG cells is influenced by the heat transfer rate across the cells. Therefore, the temperature difference between the hot and cold sides of the TEG cells would dictate the heat transfer rates across the cells, and subsequently, the generated electrical power outputs. In order to achieve this, active cooling is needed at the cold-side heat sink where the waste heat is transferred to a low temperature air stream at a reference condition of 27°C and 0.7 m/s [5]. The heated air stream enters the proofing oven at elevated temperatures where a high pre-heating degree indicates better waste heat utilization. Forced convection mechanics is dominant at both heat sinks.

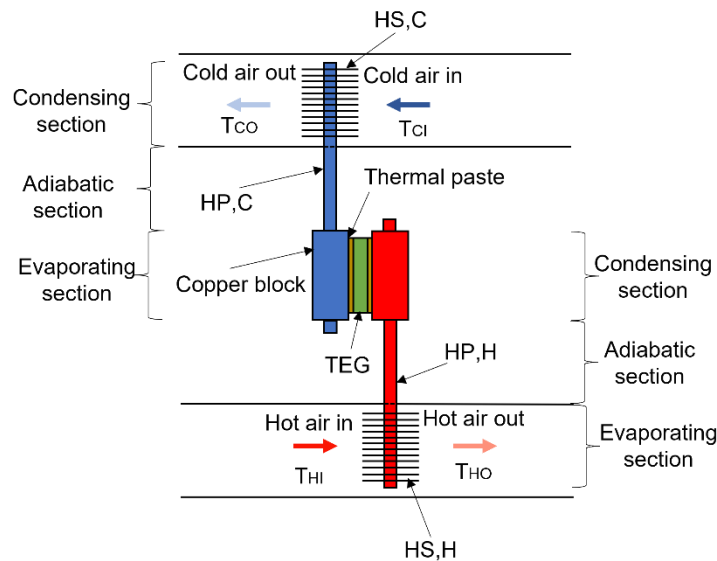


Figure 4. Operation of TEM for CHP purposes

2.2 System domain and meshing

The effectiveness of heat pipe depends on the thermal conductivity where higher thermal conductivity would enable rapid heat transfer with minimum heat loss. Wickless heat pipes with no capillary internal structure depends on gravity in transferring the condensed working fluid back to the evaporator section. CFD simulation is used to find the thermal conductivity of heat pipe for future design purposes. In the CFD model, the heat pipes are modelled as solid rods due to the complex internal structure of the component. Furthermore, modelling of heat pipes involves a multiphase fluid flow where boiling and condensation occur simultaneously and repeatedly. By changing the modelling method to solid rods, the internal behaviour and circumstances could not be well-analysed since the evaporating and condensing of the working fluid are not considered. The thermal conductivity of heat pipes is varied from 300 W/m.K until 600 W/m.K while the thermal conductivity of TEG is maintained at 1.6 W/m.K, and the results are compared with experimental data for validation. Different modelling method affects the numerical outcome due to dissimilar working flow of the system. Therefore, in this study, comparison between experimental and numerical values is thoroughly compared to ensure the reliability of the simplified model developed. Other components of the numerical TEM model are built according to the actual TEM design and specifications.

ANSYS Fluent programme is utilized in order to carry out the computational fluid dynamics (CFD) analysis. The designing and modelling of the TEM are made in Ansys SpaceClaim, as shown in Figure 5. The full model is based on the parameters of an actual physical test bench for TEM operation. The system consists of separate hot and cold fluid airflows, represented by the enclosures. The enclosure fully encloses the TEM heat sinks, and the enclosure substance is defined as air. The complete model and domain of the fluid streams are shown in Figure 5.

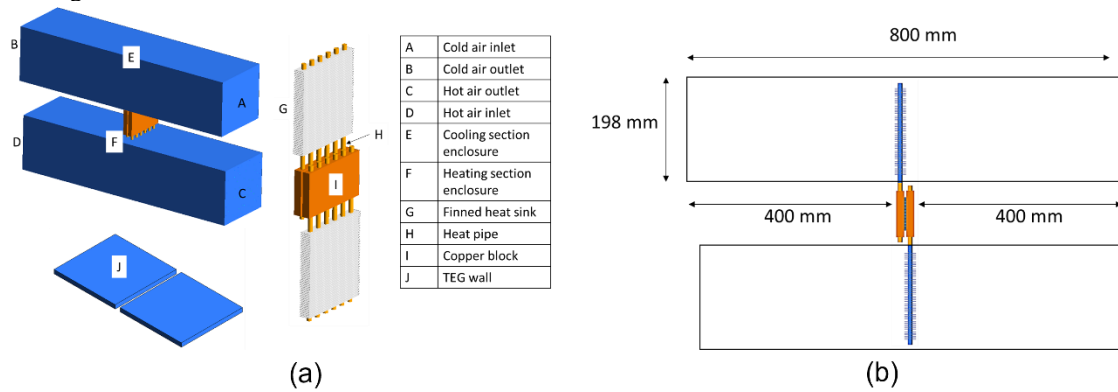


Figure 5: (a) Thermoelectric Generator Module (TEM) Model Named Selection, and (b) Domain of Fluid Streams Ducting Enclosure

The details for the meshing are provided in Table 2 and the full meshing generated for the TEM is shown in **Figure 6**, where 3.6 million elements are present in the mesh model covering the hot air until the cold air domains. The overall average skewness value for TEG module is 0.34 and the orthogonal quality average value is 0.67. Based on the skewness mesh metric spectrum, the model is in very good scale while the orthogonal quality is in a good scale. Overall, the mesh model is acceptable and can be used for simulation analysis.

Table 2: Details of the meshing setup

Domain	No. of Nodes	No. of Elements
Copper block	96606	474567
Enclosure	611379	2788529
Finned heat sinks	173474	73831
Heat pipes	311181	277840
TEG cells	3248	1512
Total	1195888	3616279
Skewness value		0.34
Orthogonal quality average		0.67

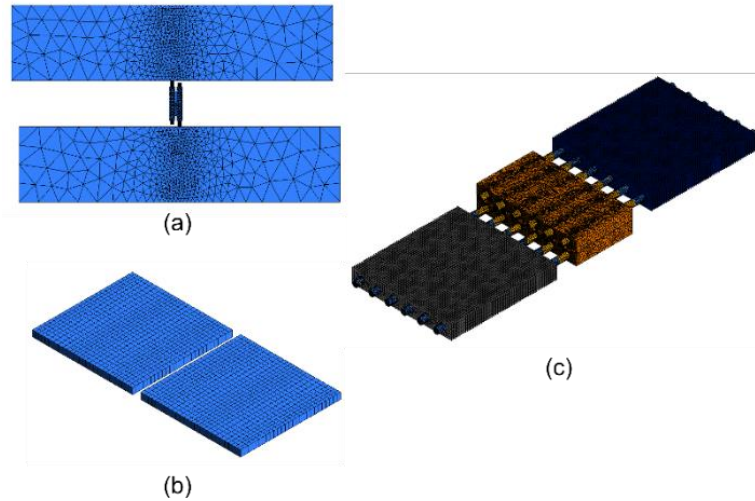


Figure 6. Mesh scheme for the TEM (a) Enclosure, (b) Thermoelectric Generator (TEG) cells and (c) Complete TEM design system

2.3 Numerical formulations

In this study, few assumptions are considered which include:

- The fluid flow is in single phase, incompressible and in steady state conditions,
- The flow is turbulent,
- Three-dimension fluid-solid conjugate is considered, and
- All physical properties of coolant air depend on its mean temperature.

The Navier-Stokes equations across x, y and z directions are given as set of Equation (1-3).

$$\rho \frac{Du}{Dt} = \rho g_x - \frac{\partial p}{\partial x} + \mu \left(\frac{\partial^2 u}{\partial x^2} + \frac{\partial^2 u}{\partial y^2} + \frac{\partial^2 u}{\partial z^2} \right) \quad (1)$$

$$\rho \frac{Dv}{Dt} = \rho g_y - \frac{\partial p}{\partial y} + \mu \left(\frac{\partial^2 v}{\partial x^2} + \frac{\partial^2 v}{\partial y^2} + \frac{\partial^2 v}{\partial z^2} \right) \quad (2)$$

$$\rho \frac{Dw}{Dt} = \rho g_z - \frac{\partial p}{\partial z} + \mu \left(\frac{\partial^2 w}{\partial x^2} + \frac{\partial^2 w}{\partial y^2} + \frac{\partial^2 w}{\partial z^2} \right) \quad (3)$$

where ρ is fluid density, u , v and w are the fluid velocity with the velocity components in three directions and p is pressure.

The energy equation is given by Equation (2) and (3).

$$\nabla \cdot (C_p \rho \vec{U} T) = k \nabla^2 T \quad (4)$$

where k is the thermal conductivity, T is the temperature and C_p is the specific heat. while the energy equation for conduction through solid is given by

$$\nabla^2 T = 0 \quad (5)$$

A sequential technique is utilized to solve the momentum and continuity equations. Due to the nonlinearity of the governing equations, the solution loop is iterated numerous times to obtain a convergent solution. The continuity, momentum, and energy equations are solved using the finite volume method, in which the integral version of the governing equations is solved using a continuum approach. The mathematical equations to describe temperature, pressure, and velocity are obtained in this manner. The convergence for momentum, mass and energy imbalance of lesser than 10^{-6} is adopted.

2.4 Solver setting

Before beginning the simulation, the gravitational acceleration along the Z-axis is adjusted to 9.81 metres per second, and all of the input values are logged in Table 3. In addition, as can be seen in Table 4, this particular arrangement of the experiment makes use of a variety of material qualities. In this particular scenario, the property of the fluid that has been prioritised is its air content. In the boundary conditions setup, the inlet temperature and

velocity for both hot and cold fluid streams are applied to the domain selected to set the starting of the fluid flow. For both hot and cold air streams, the temperatures applied to the inlet of the domain are 70°C and 20.7°C with equal velocity of 0.7 m/s. The thermal conductivity of all 12 heat pipes ranges between 300 – 600 W/m.K and the values are set to the wall of the heat pipes.

Table 3: Input solver parameters

Input parameters	Specifications	Descriptions/Values
Setup-Solver	Type	Pressure-Based
	Velocity Formulation	Absolute
	Time	Steady
Setup-Models	Energy	On
	Viscous Model	Realizable k-epsilon and standard wall treatment
	Scheme	Coupled
Solution-Methods	Flux Type	Rhie-Chow: distance based
	Gradient	Least Square Cell Based
	Pressure	Second Order
	Turbulent Kinetic Energy	Second Order Upwind
Solution-Initialization	Energy	Second Order Upwind
	Initialization Methods	Hybrid Initialization

Table 4: Material properties of the TEM components

Properties/Material	Density, ρ (kg/m ³)	Specific heat, Cp (J/kg.K)	Thermal conductivity, k (W/m.K)
TEG (Bismuth Telluride)	7640	154.5	1.6
Copper heat pipe	8978	381	300 – 600
Aluminium heat sink	2719	871	202.4
Copper block	8978	381	400

3.0 RESULTS AND DISCUSSION

3.1 Experiment temperature distribution profile

Shown in Figure 7 is the experimental temperature distribution of every component of the TEM with respect to the dimensionless length of the overall test bench. Generally, the temperature of the TEM decreases between both heat sinks due to the internal heat transfer resistance of each component. The temperature drop magnitude depends on the ability of each material to transfer heat. Lower thermal conductivity causes larger temperature difference on the local component and affects the heat transfer rate globally.

The supplied heat source is 70°C (at $x/L=0$), but the hot air temperature approaching the heat sink (at $x/L=0.3$) is only at 62°C due to heat loss through the walls. Subsequently, the complex mechanics of forced convection on the fins-hot air interface limit the average temperature of the $T_{HS,H}$ fins at 58°C. This can be improved by revising the dimensions of the fins to allow a greater hydrodynamic length and minimize flow resistance between the fins. Then, heat transfer along the heat pipes occurs by condensation and boiling to the hot-side surface of the TEG. The temperature of the $T_{TEG,H}$ is 51°C, where the 7°C temperature difference is an indicator of the low heat transfer efficiency of the wickless heat pipes. Theoretically, an efficient heat pipe would allow heat to be transferred with minimal loss that can be measured by near similar temperatures at both ends of the heat pipe. Then, the temperature difference between the TEG surfaces is approximately 10°C, dictated mainly by the thermal conductivity of the semiconductor and the effective cooling rate at the cold-side heat sink. The temperature difference between the heat pipe and the cold-side heat sink is approximately 7°C. Again, this indicates a poor heat transfer rate along the wickless heat pipe. Finally, the heat is dissipated to the cold air stream, increasing the temperature by only 2°C from its initial 23°C free stream temperature. The small increment is largely due to the low cold-side heat sink temperature that can be related to the poor efficiency of the wickless heat pipes.

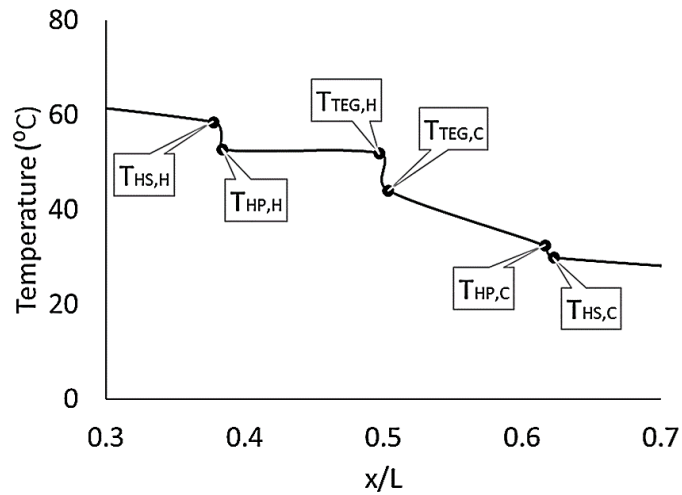


Figure 7. Dimensionless temperature profile of the TEM

3.2 Thermal conductivity of heat pipe, k_{HP}

Figure 8 shows the local temperature contour of both hot and cold surfaces of TEG cells, as the thermal conductivity of heat pipes are set to 500 W/m.K. The temperature difference on both surfaces of TEG cells is evident and the contour projects an approximately uniform temperature distribution, indicating that the simulation has reached a steady state condition and the calculation is considered converged. Figure 9 shows the global temperature contour of the TEM system. The complete model visualizes the temperature distribution of the TEM module domain and it shows the model is capable of simulating the heat transfer across all the components as a result of the temperature difference between the hot and cold air streams.

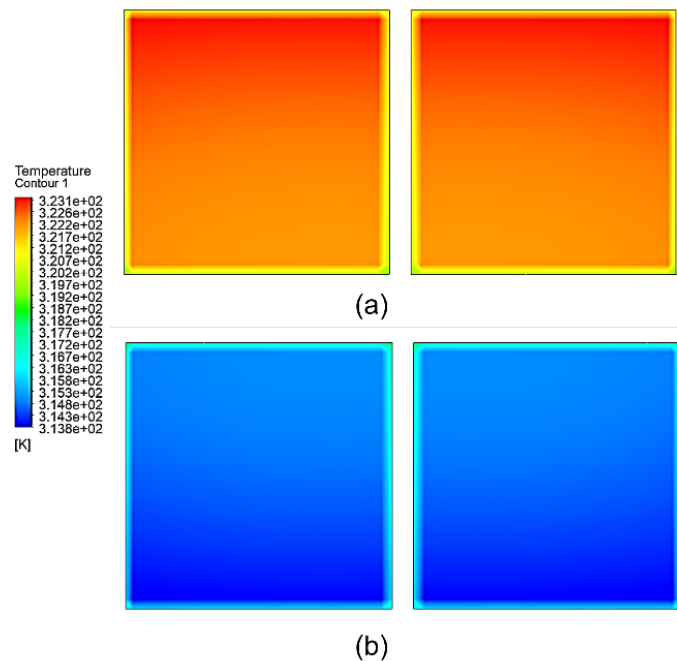


Figure 8. Temperature contour on (a) TEG hot surface and (b) TEG cold surface for case $k_{HP}=500$ W/m.K

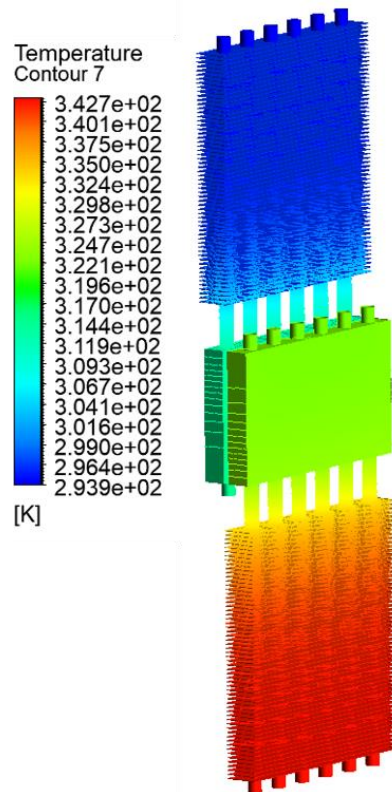


Figure 9. Global temperature distribution of the TEM system in CFD modelling

To determine the representative thermal conductivity of the wickless heat pipe, the computational variable is the heat pipe thermal conductivity from 300 -600 W/m.K. The results from the simulation is compared to the experimental data. Validation of the CFD model and the determination of the representative k_{HP} are concurrently performed, which are based on errors between the temperature of the hot and cold TEG surfaces ($T_{TEG,H}$ and $T_{TEG,C}$) and temperature difference between the TEG surfaces (ΔT).

Figure 10 displays the effect of varying the k_{HP} . Referring to the experimental data, the $T_{TEG,H}$ and $T_{TEG,C}$ are 51°C and 41°C respectively. The simulation results yield a non-linear trend for the $T_{TEG,H}$ where the temperatures at $k_{HP}=300, 500$ and 600 W/m.K have less than 5% difference with experiment results (refer Figure 11), whereas the temperature at $k_{HP}= 400$ W/m.K is 15% lower than the experiment results. However, the results for $T_{TEG,C}$ are more consistent, where the temperatures for all variations in k_{HP} is less than 5%. One of the major cause of error in numerical modelling is the number of mesh generated for a model. A multi-component model requires smaller mesh size to ensure accurate numerical calculation. Smaller mesh size increases the number of mesh in a complete model. Higher mesh number takes longer time for the numerical calculation to reach convergence. Additionally, the TEM system consists of heat sinks with very thin fins that are supposedly to require mesh refinement to accurately resolve high gradient area of the fins. However, mesh refinement is not applied to the model due to software and computer limitations. This may be the cause of non-linear trend of $T_{TEG,H}$, $T_{TEG,C}$ and ΔT .

To identify the best representative heat pipe thermal conductivity, the percentage error for the ΔT is calculated. At $k_{HP}= 500$ W/m.K, the percentage errors for ΔT is the lowest at 3%, whereas at $k_{HP}= 300$ W/m.K, the error for ΔT is approximately 30%, at $k_{HP}= 400$ W/m.K, the error for ΔT is approximately 110%, and at $k_{HP}= 600$ W/m.K, the error for ΔT is 15%. From these simulations, the identified representative thermal conductivity value for the heat pipes is 500 W/m.K.

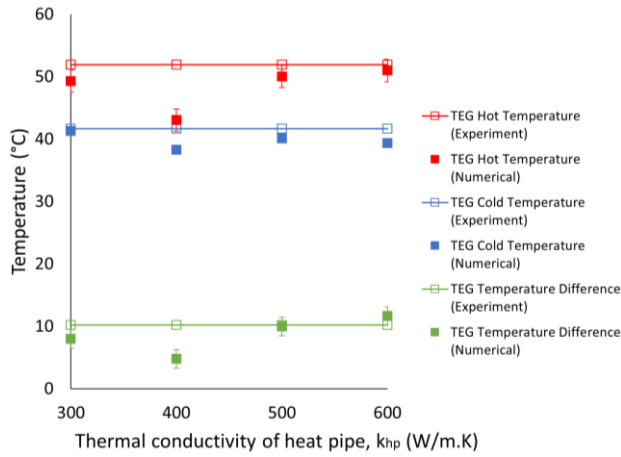


Figure 10. Experimental and numerical comparison for TEG hot and cold surfaces temperature

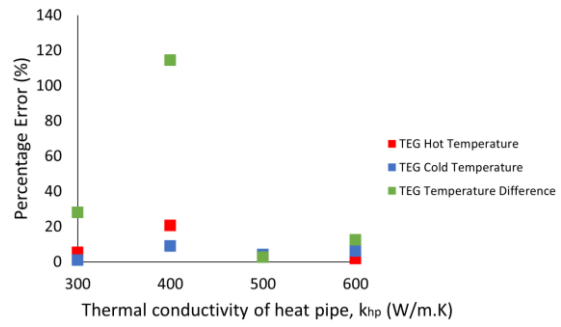


Figure 11. Percentage error for $T_{TEG,H}$, $T_{TEG,C}$ and ΔT under different k_{HP}

4.0 CONCLUSION

In this study, a computational numerical model of a TEM system is developed according to the specifications and operating conditions of an actual test bench. Heat pipes are modelled as solid rods without considering the internal structure and fluid flow. Four different thermal conductivities of heat pipe are applied to the computational modelling to find the representative value for the specific TEM system reported. The result is justified by comparing the numerical outcome with the experimental output. The value of k_{HP} is varied between 300 W/m.K until 600 W/m.k with k_{TEG} being maintained at 1.6 W/m.K. The main outcomes to be validated are the temperature of TEG for hot and cold surfaces ($T_{TEG,H}$ and $T_{TEG,C}$) and the temperature difference between the TEG surfaces (ΔT). The acceptable value of k_{HP} is found to be 500 W/m.K, with the percentage error below than 5% for all primary outcomes. Acquiring the representative thermal conductivity of heat pipe is useful for mathematical analysis where it replaces the heat transfer coefficient that requires thorough understanding on internal boiling and condensation principle. Besides, the computational model developed and the simplified method used are applicable for future TEM designing as it consumes less computational time. Therefore, by conducting CFD simulations and obtaining the representative value of the thermal conductivity, future complex modelling could be avoided as simplified model is sufficient in numerical approach.

REFERENCES

- [1] M. Hamid Elsheikh et al., “A review on thermoelectric renewable energy: Principle parameters that affect their performance,” *Renew. Sustain. Energy Rev.*, vol. 30, pp. 337–355, 2014, doi: 10.1016/j.rser.2013.10.027.
- [2] B. I. Ismail and W. H. Ahmed, “Thermoelectric power generation using waste-heat energy as an alternative green technology,” *Recent Patents Electr. Eng.*, vol. 2, no. 1, pp. 27–39, 2009, doi: 10.2174/1874476110902010027.
- [3] M. F. Remeli, L. Tan, A. Date, B. Singh, and A. Akbarzadeh, “Simultaneous power generation and heat recovery using a heat pipe assisted thermoelectric generator system,” *Energy Convers. Manag.*, vol. 91, pp. 110–119, 2015, doi: 10.1016/j.enconman.2014.12.001.
- [4] R. Venkatasubramanian, E. Siivola, T. Colpitts, and B. O’ Quinn, “Thin-film thermoelectric devices with high room-temperature figures of merit,” *Mater. Sustain. Energy A Collect. Peer-Reviewed Res. Rev. Artic. from Nat. Publ. Gr.*, pp. 120–125, 2010, doi: 10.1142/9789814317665_0019.
- [5] M. H. Hamdan, N. A. Mat Som, A. Abdul Rashid, and G. J. Jimmy, “Performance analysis on series and parallel circuit configurations of a four-cell thermoelectric generator module design,” *J. Appl. Eng. Des. Simul.*, vol. 1, no. 1, pp. 32–42, 2021, doi: 10.24191/jaeds.v1i1.18.
- [6] A. Baroutaji et al., “Advancements and prospects of thermal management and waste heat recovery of PEMFC,” *Int. J. Thermofluids*, vol. 9, p. 100064, 2021, doi: 10.1016/j.ijft.2021.100064.
- [7] S. J. G. Cooper, G. P. Hammond, and J. B. Norman, “Potential for use of heat rejected from industry in district heating networks, Gb perspective,” *J. Energy Inst.*, vol. 89, no. 1, pp. 57–69, 2016, doi: 10.1016/j.joei.2015.01.010.
- [8] A. K. Reji, G. Kumaresan, N. Kaushik, V. S. Navin Karthi, and M. K. Naveen, “Thermal analysis of grooved heat pipe with eco-friendly refrigerant for low heat loads in comparison to an ordinary thermosyphon,” *Mater. Today Proc.*, vol. 66, pp. 878–882, 2022, doi: 10.1016/j.matpr.2022.04.512.
- [9] M. Mahdi, J. Abdulateef, A. M. Abdulateef, M. Sabah Mahdi, and A. M. Abdulateef, “Thermoelectric Combined Heat and Power Generation System Integrated with Liquid-Fuel Stove Enhancement of Phase

- Change Materials View project Thermal energy storage View project Thermoelectric Combined Heat and Power Generation System Integrated with Liquid-Fuel Stove,” *J. Adv. Res. Fluid Mech. Therm. Sci. J. homepage*, vol. 51, pp. 19–30, 2018, [Online]. Available: www.akademiabaru.com/arfmts.html.
- [10] Y. Zhang, X. Wang, M. Cleary, L. Schoensee, N. Kempf, and J. Richardson, “High-performance nanostructured thermoelectric generators for micro combined heat and power systems,” *Appl. Therm. Eng.*, vol. 96, pp. 83–87, 2016, doi: 10.1016/j.applthermaleng.2015.11.064.
- [11] S. Zarifi and M. Mirhosseini Moghaddam, “Utilizing finned tube economizer for extending the thermal power rate of TEG CHP system,” *Energy*, vol. 202, Jul. 2020, doi: 10.1016/j.energy.2020.117796.
- [12] W. J. Zou, K. Y. Shen, S. Jung, and Y. B. Kim, “Application of thermoelectric devices in performance optimization of a domestic PEMFC-based CHP system,” *Energy*, vol. 229, Aug. 2021, doi: 10.1016/j.energy.2021.120698.
- [13] M. Saufi Sulaiman, B. Singh, and W. A. N. W. Mohamed, “Experimental and theoretical study of thermoelectric generator waste heat recovery model for an ultra-low temperature PEM fuel cell powered vehicle,” *Energy*, vol. 179, pp. 628–646, 2019, doi: 10.1016/j.energy.2019.05.022.
- [14] N. F. Zamri, M. H. Hamdan, S. N. A. Anuar, W. A. N. W. Mohamed, and M. F. Remeli, “Performance of a Plate-Finned Thermoelectric Generator (TEG) Module for Industrial Waste Heat Recovery,” *J. Mech. Eng.*, vol. 19, no. 3, pp. 257–272, 2022, doi: 10.24191/jmeche.v19i3.19817.